Journal Name

ARTICLE TYPE

Cite this: DOI: 00.0000/xxxxxxxxxx

Black phosphorus mediated Photoporation: a broad absorption nanoplatform for intracellular delivery of macromolecules †

Jielin Wang,[a,b,c,d] Aranit Harizaj,[d] Yongbo Wu,[a,b,c] Xiaofang Jiang,[a,b,c] Toon Brans,[d] Juan C. Fraire,[d] Julián Mejía Morales,[d] Stefaan C. De Smedt,[d] Zhilie Tang,[*a,b,c] Ranhua Xiong4,[*d,f] and Kevin Braeckmans[*d,e]

Received Date
Accepted Date

DOI: 00.0000/xxxxxxxxxx

Nanoparticle-sensitized photoporation for intracellular delivery of external compounds usually relies on the use of spherical gold nanoparticles as sensitizing nanoparticles. As they need stimulation with visible laser light, they are less suited for transfection of cells in thick biological tissues. In this work, we have explored Black Phosphorus Quantum Dots (BPQD) as alternative sensitizing nanoparticles for photoporation with a broad and uniform absorption spectrum from the visible to the Near Infra-Red (NIR) range. We demonstrate that BPQD sensitized photoporation allows efficient intracellular delivery of We demonstrate that BPQD sensitized photoporation allows efficient intracellular delivery of both siRNA (>80%) and mRNA (>40%) in adherent cells as well as in suspension cells. Cell viability remained high (>80%) irrespective whether irradiation was performed with visible (532nm) or near infrared (800nm) pulsed laser light. Finally, as a proof of concept, we used BPQD sensitized photoporation to deliver macromolecules in cells with a thick phantom tissue in the optical path. NIR laser irradiation resulted in only 1.3× reduction in delivery efficiency as compared to photoporation without phantom gel, while with visible laser light the delivery efficiency was reduced 2×.

Intracellular delivery technologies have become indispensable in biomedical research[1], whether it is for modifying cell behavior with nucleic acids or proteins, or for imaging of cells with contrast agents. However, especially when working with primary hard-to-transfect cells, it remains a challenge to deliver such extrinsic compounds with high efficiency, and low cytotoxicity into the cytosol of cells. So far, biological, chemical and physical methods have been developed to achieve delivery of macromolecules across the cell membrane. Toxicity and immunogenicity of viral vectors are a major disadvantage of biological methods, apart from the fact that they are only suited to deliver nucleic acids[2]. Chemical vectors, including polymers and lipids, have a better safety profile but often lack in efficiency on primary and 'hard-to-transfect' cells[3]. This is why substantial efforts have gone into developing physical methods like microinjection[4,5], electroporation[6–8], biolistics[9,10] ,magnetofection[11] and sonoporation[12]. They all have in common that they use a physical trigger or force to perturb the cell membrane, allowing active or passive entry of external molecules inside cells. Especially for in vitro or ex vivo applications, such as for the production of engineered cells, physical methods have proven to be broadly applicable to many cell types and a wide range of macromolecules. Striving for ever better intracellular delivery efficiencies with minimal cell toxicity, nanoparticle sensitized photoporation has emerged as a particularly promising upcoming physical intracellular delivery method. With pulsed laser irradiation, photothermal nanoparticles can generate thermal and mechanical effects that induce transient permeabilization of the cell membrane.[13]. Even though femto- and picosecond laser pulses have been successfully used[14–18], most studies rely on nanosecond pulsed lasers, which are far more affordable for the same power output[13,19–22]. Traditionally, gold nanoparticles (AuNPs) have been used the most as photothermal sensitizers, which can be efficiently excited within their relatively narrow plasmon extinction peak (520-565 nm), for instance with a Q-switched DPPS laser at 532 nm[23]. While irradiation in the visible spectrum is perfectly fine for intracellular delivery

[a] School of Physics and Telecommunication Engineering, South China Normal University, Guangzhou, 510006, China.
[b] Guangdong Research Center of Photoelectric Detection Instrument Engineering Technology, Guangzhou,510006, China.
[c] Guangdong Provincial Key Laboratory of Quantum Engineering and Quantum Materials, Guangzhou,510006, China.
[d] Laboratory of General Biochemistry and Physical Pharmacy, Faculty of Pharmaceutical Sciences, Ghent University, Ottergemsesteenweg 460, Ghent 9000, Belgium. Fax: +32 (0)9 264 81 89; Tel:+32 (0)9 264 80 98; E-mail: Kevin.Braeckmans@UGent.be
[e] Centre for Advanced Light Microscopy, Ghent University, Belgium.
[f] Joint Laboratory of Advanced Biomedical Materials (NFU-UGent), International Innovation for Center for Forest Chemicals and Materials, College of Chemical Engineering, Nanjing Forestry University (NFU), Nanjing 210037, P. R. China.

in monolayers of cells, in thicker tissues it would be preferrable to move to longer wavelengths in the first biological transparency window (650-950 nm) where less light scattering and absorption occurs[24]. Since spherical AuNP have low light absorption in that region, gold nanorods have been suggested instead[25]. They are, however, more difficult to synthesize and require potentially toxic reagents such as CTAB[26,27].

To extend nanoparticle sensitized photoporation towards excitation in the NIR range, in this work we explore the use of Black Phosphorus (BPQD) nanoparticles which have an extremely broad and uniform absorption spectrum across the visible and NIR range with high photothermal conversion efficiency and good biocompatibility[28]. In addition, their 2D lamellar structure offers the possibility for further functionalization to improve, for instance, cell membrane attachment and intracellular delivery efficiency. First, we synthesize Black Phosphorus Quantum Dots (BPQD) functionalized with the cationic polymer polyethyleneimine to enhance adsorption to the negative cell membrane via electrostatic interaction. The BPQD are characterized in terms of extinction spectrum, size, zeta potential and morphology. Next we investigate their suitability to deliver a broad range of macromolecular compounds, including mRNA, by photoporation in adherent (HeLa) and suspension (Jurkat cells) cells. Finally, we explore if BPQD enable enhanced photoporation efficiency through a 2 mm thick phantom tissue with NIR pulsed laser excitation. In summary, this study performed BPQDs mediated Photoporation as a more broadly application system for macromolecule intracellular delivery, which is also expected to extend in vivo photoporation in the future.

1 Results

1.1 Synthesis and characterization of black phosphorus quantum dots

BPQD were synthesized by liquid stripping of bulk BPQD as reported before[29?] . The UV-vis absorption spectrum was measured for different concentrations of BPQD. As expected, the BPQD were found to have an almost uniform extinction spectrum from 250 nm to 850 nm (Fig. 1a). Even though the extinction spectrum has a scattering component to it, this suggests that any excitation wavelength in this range could likely be used for photoporation. Transmission electron microscopy (TEM) showed that the BPQD had a circular shape with a size of 20.2 ± 5.1 nm (Fig 1b). Next, the BPQD suspension was irradiated with 532 nm pulsed laser light (5 ns pulses) and 800 nm pulsed laser light (2 ps pulses). The laser beam was scanned across the sample such that each position was illuminated with a single laser pulse. When measuring the UV-vis spectrum afterwards, it was noticed that the absorption spectrum had decreased onwards from 400 nm (Fig. 1c). The decrease in absorption was proportional to the applied laser pulse fluence, irrespective of the type of laser irradiation. This is an indication that BPQD undergo structural changes upon pulsed laser irradiation. It has been previously reported that BPQD can degrade into biocompatible substances like $PO2^{3}-$,$PO3^{3}-$ and $PO4^{3}-$ upon laser irradiation[30,31]. This is in line with our observation that the pH of BPQD in ddH2O decreased proportionally to the applied laser pulse fluence (Fig. 1d). Importantly, in the absence of laser irradiation, the BPQD stored at 4°C remained stable in water for at least 4 months (Fig. S1).

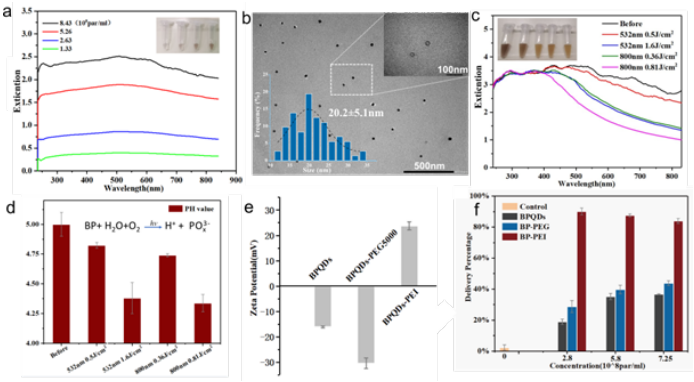

Fig. 1 Characterization of BPQD. (a) UV-Vis absorption spectra of BPQD for various concentrations in water (8.43, 5.26, 2.63 and 1.33 × 10^9 particles/mL); (b) Representative TEM image and size distribution of BPQD; (c) UV-Vis extinction spectra of BPQD before and after irradiation with 532 nm laser lights of 5 ns pulses (0.11and 0.33 J/cm²), and with 800 nm laser light of 2 ps pulses (0.08 and 0.17 J/cm²); (d) The pH of BPQD dispersed in ddH2O before and after laser irradiation; (e) The Zeta potential of pristine BPQD, and BPQD after pegylation (BPQD-PEG) or coating with polyethyleneimine (BPQD-PEI); (f) Comparison between BPQD, BPQD-PEG and BPQD-PEI for FD10 delivery in Hela cells by photoporation.

1.2 Surface functionalization of BPQD and photoporation efficiency

Next, BPQD were further functionalized with polyethylene glycol (PEG) or the cationic polymer polyethyleneimine (PEI, 25kDa). The zeta potential of pristine BPQDs in water was -16.1 mV, which changed to -30.4 mV after PEGylation or +23.8 mV after coating with PEI (Fig. 1e). Next, BPQD, BPQD-PEG and BPQD-PEI were used for photoporation experiments on adherent HeLa cells. The particles were incubated with Hela cells for 30 mins at increasing concentrations (2.8, 5.8 and 7.25×10^8 part/ml), after which cells were washed and supplemented with fresh cell culture medium containing 2 mg/ml FITC-dextran of 10 kDa (FD10). FD10 was chosen as model macromolecule whose intracellular delivery can be easily quantified by flow cytometry. Cells were subsequently irradiated with pulsed laser light (532 nm, 5 ns, 0.11 J/cm^2). When determining the percentage of FD10 positive cells by flow cytometry, it is clear that BPQD-PEI provided the highest delivery efficiency, with >90% positive cells for 2.8×10^8 part/ml (Fig. 1f). Pristine and PEGylated BPQD clearly yielded lower delivery efficiencies for the same nanoparticle concentrations. This is most likely due to better adhesion of the cationic BPQD-PEI to the negatively charged cell membrane. Even though photoporation with BPQD-PEI was more toxic at the concentrations tested here (Fig. S2), it was decided to continue from here on with BPQD-PEI, knowing that cell viability can be improved by fine-tuning of the particle concentration, which will be done in the next section.

1.3 Photoporation with BPQD-PEI using visible and NIR laser wavelengths

Next, we wanted to verify if intracellular delivery can be achieved with both visible and NIR irradiation. First, we optimized PEI-BPQD concentration for optimal delivery of FD10 in HeLa's with 532 nm laser pulses (5 ns, 0.11 J/cm²) (Fig. 2a). As expected, the delivery efficiency increases with particle concentration at the expense of cell viability which was measured 2 h after photoporation with the Cell Titer-Glo metabolic assay. For the highest particle concentration (2×10^8 par/ml) 80% positive cells were obtained with 80% cell viability. The same experiment was then repeated with 800 nm laser pulses (2 ps, 0.08 J/cm²). Again we found that delivery efficiency increased with increasing particle concentrations (Fig. 2b), but with a concomitant decrease in cell viability (Fig. 2c). An increasing delivery efficiency for higher particle concentrations can also be visually appreciated from the representative confocal images in Fig. S3a. Again 80% positive cells with 80% viability was obtained with 800 nm laser irradiation (0.08 J/cm²) for the highest particle concentration (2×10^8 part/ml), showing that BPQD enable equally efficient photoporation of cells irrespective of the wavelength used.

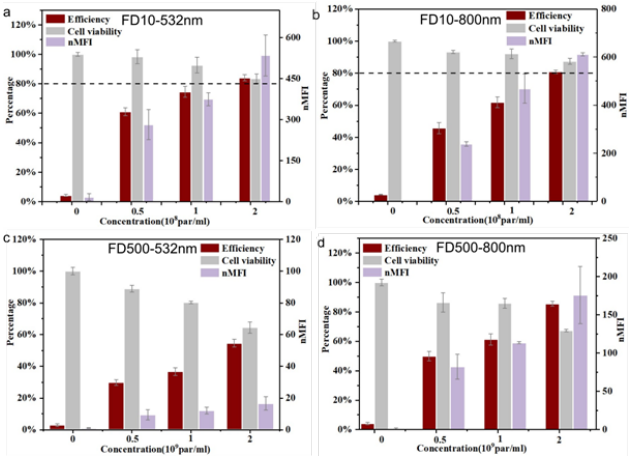

Fig. 2 Photoporation of Hela and Jurkat cells with PEI-BPQD using different laser wavelengths. (a) Evaluation of FD10 delivery efficiency (% positive cells) and rMFI in HeLa cells by flow cytometry. Cell viability was measured 2 hours after photoporation. Photoporation was performed with a 532 nm laser (5 ns, 0.11 J/cm²) using PEI-PB at a concentration of 0, 0.5, 1, 2 and 10^8 par/ml. (b) FD10 delivery efficiency in Hela cells by photoporation with a 800 nm laser (2 ps, 0.08 J/cm²). (c) Evaluation of FD500 delivery efficiency and rMFI in Jurkat cells as measured by flow cytometry. Cell viability was measured 2 hours after photoporation. Photoporation was performed with a 532nm laser (5 ns, 0.11 J/cm²) using PEI@BPQD at a concentration of 0, 0.5, 1, 2 and 10^9 par/ml. (d) FD500 delivery efficiency in Jurkat cells by photoporation with 800 nm laser irradiation (2ps, 0.08 J/ cm²) using PEI@BPQD at a concentration of 0, 0.5, 1, 2 and 10^9 par/ml.

Next, we tried to deliver FD500 into difficult to transfect Jurkat suspension cells, which is a frequently used model cell line for hard-to-transfect T cells. With 532 nm laser irradiation (5 ns, 0.11 J/cm²), 36.7% positive cells were obtained with 80% cell viability at 1×10^9 par/ml (Fig. 2d), while for 800 nm irradiation (2 ps, 0.08 J/cm²) 61.3% positive cells were obtained with >80% viability at 1×10^9 part/ml (Fig. 2e). Fig. S3b shows representative confocal images after photoporation (800 nm, 0.08 J/cm²) for increasing BPQD-PEI concentrations (0, 0.5, 1 and 2 $\times10^9$ par/ml). It is surprising that with 800 nm laser irradiation the delivery efficiency of FD500 was better than for 532 nm irradiation, while this was not the case for FD10. Presumably this is due to differences in photothermal phenomena generated with 5 ns pulses at 0.11 J/cm² as opposed to 2 ps pulses at 0.08 J/cm². Indeed, it was shown before that ps laser pulses are more efficient than ns pulses in heating of nanoparticles and VNB formation due to better heat confinement[32]. As it leads to a higher temperature in the nanoparticles for the same laser fluence, ps laser irradiation is more likely to induce the generation of water vapor nanobubbles, while with ns laser pulses of a similar fluence only heat will be generated. While heated nanoparticles can permeabilize the cell membrane, VNB can form bigger pores in the cell membrane[13]. Even though this may not make a difference for fairly small macromolecules such as FD10, it could affect the intracellular delivery of large macromolecules such as FD500.

1.4 Cell transfections with siRNA and mRNA

Next we wanted to verify if photoporation with PEI-BPQD can be used to deliver actual functional biological molecules into cells. For the optimized conditions based on FD10 delivery in adherent HeLa cells with 532 nm laser irradiation, we transfected H1299-eGFP cells with eGFP-siRNA, of which exemplary confocal images are shown in Fig. 3a. Untreated H1299-eGFP cells constitutively express eGFP, which did not change when cells were incubated with siRNA and PEI-BPQD (without laser irradiation) or with siRNA and laser irradiation (without PEI-BPQD). However, after BQPD sensitized photoporation in the presence of eGFP-siRNA, eGFP fluorescence clearly diminished after 24 h, even for the lowest siRNA concentration of 0.5 μM. A clear decrease in eGFP expression was also observed by flow cytometry (Fig. 3b), reaching 75% knock-down efficiency for 0.5 μM siRNA and increasing slightly to 80% for 2 μM siRNA. Cell viability, measured by CellTiter-Glo after 24h, remained 90-100% in all cases. This shows that efficient functional transfections are very well possible with BPQD sensitized photoporation.

Next, we tried transfecting Jurkat cells with mRNA, which has a molecular weight of the same order as FD500. Since we obtained the best delivery efficiency for FD500 with 800 nm 2ps laser pulses, we continued with the optimized conditions for that laser. As can be seen in the exemplary confocal images in Fig. 4a, both the percentage of eGFP transfected cells and the amount of eGFP expression increased with increasing mRNA concentration (0.1-0.4 ug/ml) 24 h after photoporation. Quantification by flow cytometry showed about 40% positive cells for an mRNA concentration of 0.1 ug/ml. The transfection efficiency increased to 53% when increasing the mRNA concentration to 0.4 ug/ml, although at the expense of decreased cell viability. These results once more confirm that intracellular delivery of functional molecules in cells is very well possible with PEI-BPQD sensitized photoporation, even when using NIR laser irradiation.

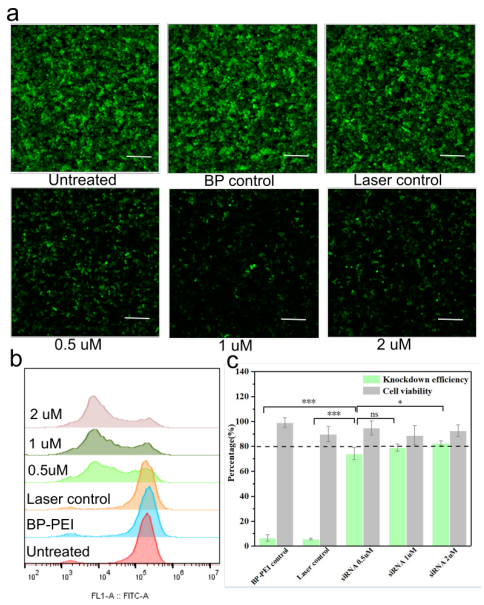

Fig. 3 HeLa cells transfected with siRNA by BPQD sensitized photoporation using 532 nm laser irradiation (0.11 J/cm², 5 ns). (a) Representative confocal images of H1299-eGFP cells without treatment, treatment with eGFP-siRNA and BPQD-PEI without laser irradiation (BPQD control), treatment with eGFP-siRNA and laser irradiation without PEI-BPQD (Laser control), and photoporated with different concentrations of eGFP-siRNA (0.5 µM, 1 µM and 2 µM). The scale bar is 100 µm. (b) Representative corresponding flow cytometry histograms. (c) Knockdown efficiency and cell viability of eGFP-siRNA photoporated cells as determined by flow cytometry and CellTiter-Glo, respectively. (n=3, ***p<0.001, *p<0.5, ns=nonsignificant).

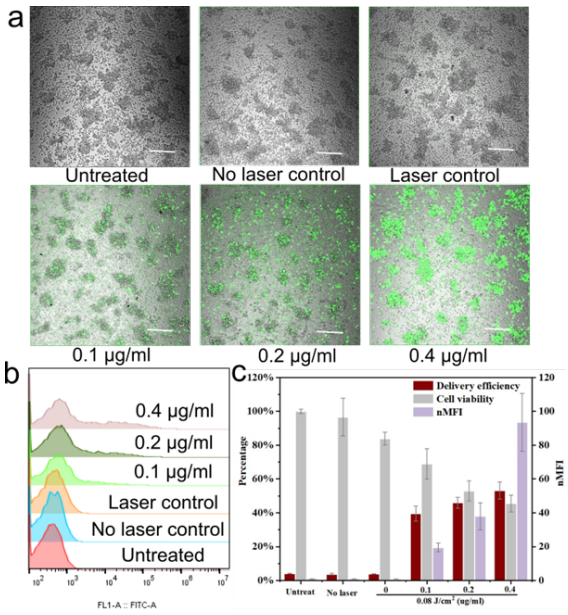

Fig. 4 eGFP-mRNA delivery into Jurkat cells by BPQD sensitized photoporation. (a) Confocal images of Jurkat cells. Top row: transmission images; Bottom row: overlay of transmission images with eGFP fluorescence images. The scale bar is 100 µm. (b) Representative corresponding flow cytometry histograms . (c) Quantification of delivery efficiency and nMFI by flow cytometry for the same conditions. Cell viability was measured by Cell Titre Glo assay.

1.5 BPQD sensitized photoporation of cells through phantom tissue

The possibility to perform BPQD sensitized photoporation at 800 nm laser irradiation should enable better cell transfections in thick tissues. To evaluate this, we photoporated HeLa cells with FD10 with a 2 mm thick phantom tissue between the laser and cells, as schematically depicted in Fig. 5a. Using 532 nm laser irradiation (0.11 J/cm²), delivery efficiency was 40% (Fig. 5b), which is 2× less of what was achieved without the phantom gel (cfr. Fig. 2a). Even when increasing the laser pulse fluence to 0.33 J/cm², only 60% positive cells could be obtained. Instead, when using 800 nm laser irradiation (0.08 J/cm²), delivery efficiency was still 60% (Fig. 5c), which is only 1.3× less as compared to photoporation without phantom gel (cfr. Fig. 2b). By increasing the laser pulse fluence to 0.26 J/cm², the delivery efficiency could be restored to nearly 80% again. Together this confirms that optical losses are indeed substantially reduced when using NIR instead of visible irradiation for photoporation.

2 Materials and methods

2.1 Nucleic acids

Twenty-one-nucleotide siRNA duplexes targeting the enhanced green fluorescent protein (siEGFP) and negative control duplexes (siCTRL) were purchased from Eurogentec (Seraing, Belgium). siEGFP: sense strand = 5'-CAAGCUGACCCUGAAGUUCtt-3'; antisense strand = 5'-GAACUUCAGGGUCAGCUUGtt-3'. siCTRL: sense strand = 5'-UGCGCUACGAUCGACGAUGtt-3'; antisense strand = 5'-CAUCGUCGAUCGUAGCGCAtt-3' (lower case bold letters represent 2'-deoxyribonucleotides, capital letters are ribonucleotides). For fluorescence experiments, the siCTRL duplex was labeled with a Cy5 dye at the 5' end of the sense strand (Eurogentec). CleanCap (cc) enhanced green fluorescent protein (eGFP) was purchased from TriLink Biotechnologies (San Diego, California, USA) and stored at -80 °C until use.

2.2 Cell culture

HeLa cells (ATCC® CCL-2™) were cultured in DMEM/F-12 (Gibco-Invitrogen, Renfrew Renfrewshire PA4 9RF, UK) supplemented with 10% heat-inactivated fetal bovine serum (FBS) (Biowest, Nuaillé, France), 2 mM glutamine (Gibco-Invitrogen), and 100 U/mL penicillin/streptomycin (Gibco-Invitrogen). Cells were passaged using DPBS (Gibco-Invitrogen, Renfrewshire PA4 9RF, UK) and trypsin-EDTA (0.25%, Gibco-Invitrogen). HeLa cells and H1299-eGFP cells were cultivated in a humidified tissue culture incubator at 37 °C and 5% CO_2. For photoporation, 2×104 Hela or H1299-eGFP cells were seeded per well of a 96 well plate (Greiner Bio-One) 24 hours before treatment. Jurkat E6-1 cells were maintained in a humidified atmosphere of 5% CO2 at 37 °C, and the culture medium was renewed every 2–4 days. For photoporation, 2.5 $\times 10^5$ Jurkat cells were seeded per well of a 96 well plate, which was immediately followed by laser irradiation. All cell culture products were purchased from Life Technologies (Renfrewshire PA4 9RF, UK), unless specifically stated otherwise.

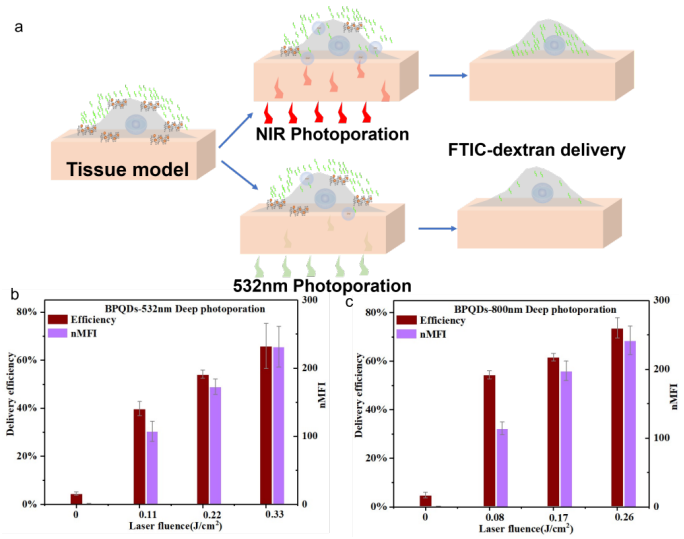

Fig. 5 Photoporation of HeLa cells in the presence of a 2 mm thick tissue model. (a) Schematic illustration of the experimental setup. (b) Efficiency and nMFI of FD10 delivery into Hela cells using 532 nm photoporation. (c) Efficiency and nMFI of FD10 delivery into Hela cells using 800 nm photoporation.

2.3 BPQD sensitized photoporation synthesis and characterization

BPQD were prepared from bulk BPQD using the liquid stripping method using sonication (Scient-IID and Scientz SB25-12DTD) for 8h at 4°C with 10-25% intensity and 3s/1s on/off intervals. UV-VIS absorption spectra were measured by a NanoDrop 2000c Spectrophotometer (ThermoFisher Scientific) for various concentrations (8.43, 5.26, 2.63, 1.33 $\times$ 10^9 particles/mL) in water. The particle concentration was measured by NanoSight (Malvern, UK). The pH value of BPQD in ddH2O before and after pulsed laser irradiation were measured with a pH meter (Consort). BPQD were further functionalized with polyethyleneglycol (PEG) and polyethyleneimine (PEI). For functionalization with PEG, BPQD were suspended in 25ml water to which 50 mg mPEG-Amine (5kDa, Creative PEGWorks, USA) was added. After half an hour bath sonication at room temperature, the solution was centrifuged at 10000 rpm for 30 min to remove free PEG. For functionalization with PEI, PEI (branched, 25kDa, Sigma, Belgium) was diluted into ultrapure water to a 10%(w/w) solution and added to the BPQD suspension, followed by sonicated for 1-2mins and stirred overnight. The solution was centrifuged at 10000 rpm for 30 min to remove free PEI, which was repeated for at least 3 times. The Zeta potential of BPQD, PEG-BPQD and PEI@BPQD were measured with a Zetasizer (Malvern, UK).

2.4 Intracellular delivery of FITC-dextrans by BPQD sensitized photoporation

FITC-dextrans of 10 kDa (FD10) and 500 kDa were purchased from Sigma. Cells were first incubated for 30 min with PEI-BPQD, washed with DPBS, and supplemented with fresh cell culture medium containing 1 mg/ml FD10 or FD500. For suspension cells a pre-centrifugation step of 350 rcf was included (5430R, Eppendorf) to let the cells settle at the bottom of the wells. Two home-built photoporation setups were used in this work, one equipped with a 5-ns pulsed laser at 532 nm and another with a 2 ns pulsed laser at 800 nm. Confocal microscopy images were recorded with a Nikon A1R confocal microscope (Nikon BeLux, Brussels, Belgium) using 488 nm laser excitation for FITC-dextran or eGFP visualization. Delivery efficiency was quantified by flow cytometry (CytoFLEX, Beckman coulter,Germany) and Flowjo software. All data are expressed as the mean ± SD (n=3).

2.5 Cell viability measurements

The CellTitre-Glo assay (CellTiter-Glo® Luminescent Cell Viability Assay, Promega, WI, USA) was used to measure cell viability. 100uL of CellTiter Glo® solution was added into each well 2h (FD10 and FD500) or 24h (siRNA and mRNA) after photoporation and shaken at 100 rpm for 5-10 mins. The luminescent signal for each well was measured by a GloMax plate reader (GloMax® 96 Microplate Luminometer, Promega, Leiden, the Netherlands).

2.6 Transfection with siRNA and mRNA by BPQD sensitized photoporation

eGFP siRNA (siEGFP) was purchased from Eurogentec (Seraing, Belgium). mRNA encoding for eGFP was obtained from TriLink Biotechnologies (San Diego, California, USA). Cells were first incubated for 30 min with PEI-BPQD, washed with DPBS, and supplemented with fresh cell culture medium containing siRNA at a concentration as indicated in the text. A similar procedure was followed for mRNA transfections except that Jurkat cells were washed at least twice with Opti-MEM before applying Opti-MEM with mRNA. These extra washing steps are needed to limit mRNA degradation by secreted RNases. In addition, the whole photoporation treatment was finished in 10 mins again to minimize mRNA degradation[20]. The siEGFP knockdown efficiency was quantified by flow cytometry from the average fluorescence intensity of the cells before and after transfection[13]: Knockdown efficiency(%)=(1-MFIsiEGFP/MFIsiCTRL)$\times$100%

2.7 BPQD sensitized photoporation of cells through phantom tissue

As a tissue model a phantom gel was prepared from 2g Agar gel, 2.5g Gelatin powder and 2.5 ml Intralipid per 100mL water. The mixture was heated to 90^0C and poured into an inverted 96 well plate to form a flat gel layer of 2 mm just below the wells. Next, HeLa cells were cultured into the 96 well plate and photoporated as described above. When placed on the photoporation setup, laser light will first pass through the 2 mm thick gel layer before reaching the cells in the wells, thus simulating the presence of thick tissue.

3 Discussion

Photoporation is a promising physical technique for safe and efficient intracellular delivery of exogenous molecules, which has been successfully applied to live-cell labeling and genetic engineering of cells[33]. While usually spherical AuNPs are used as photothermal sensitizers, they have a narrow extinction peak around 520-565 nm, making those sensitizers less suited for transfection

of cells in thick tissues due to strong optical losses for visible light. Furthermore, AuNPs tend to break up in small fragments already after the first laser pulse, giving cause for concern of genotoxicity[34].Other reported sensitizers for photoporation like carbon dots[35], graphene-based materials[19] and polymeric nanoparticles also have quite broad absorption spectra, but they quickly decay towards the NIR. Instead, BPQDs have an extended uniform absorption spectrum from the visible to the near infrared. In combination with a favorable biocompatibility profile, they offer particularly attractive properties to perform photoporation in thick biological tissues. In previous work we showed that graphene quantum dots are more stable than AuNP and can be excited at NIR wavelengths[19]. However, the biocompatibility of those materials remains uncertain, while the absorption spectrum decays substantially towards the NIR region. This is why we here investigated the use of BPQD which have a better biocompatibility profile[30?] and an almost uniform absorption spectrum from the visible to NIR wavelength range (Fig. 1a). BPQD is a two-dimensional material with special optical and electrical properties that has attracted considerable interest for bio-applications, such as cancer therapy, drug delivery and bioimaging[29,36–39]. Following successful BPQD synthesis and characterization, we found that functionalization with the cationic polymer PEI resulted in markedly better photoporation efficiencies as compared to pristine or pegylated BPQD. This is similar to what we found before for graphene quantum dots and can be ascribed to the fact that cationic particles can more efficiently adhere to the negatively charged cell membrane[40]. Using PEI-BPQD, we next demonstrated that FD10 can be equally efficiently delivered in HeLa's using 532 nm or 800 nm laser irradiation, demonstrating that BPQD can indeed be used for NIR photoporation. Delivery of FD500 was successfully achieved in Jurkat suspension cells as well, although in this case delivery efficiency was markedly better when performing photoporation at 800 nm. As already explained, this is likely due to the fact that ps laser pulses result in better thermal confinement and, therefore, are more likely to induce large membrane pores by the generation of vapor nanobubbles[33,41,42] Using optimized conditions based on FD10 delivery, we next demonstrated successful transfection of H1299 lung carcinoma cells with siRNA, resulting in 75% transfected cells for 0.5 μM siRNA. Next, using optimized conditions based on FD500 delivery, we transfected Jurkat cells with eGFP-mRNA, resulting in 40% transfected cells in case of 800 nm laser irradiation with 0.1 ug/ml mRNA. This is markedly better to what we have achieved before when using 70 nm spherical AuNPs, in which case eGFP-mRNA transfection efficiency was 20% for 0.1 ug/ml mRNA[20]. Further investigations are needed to elucidate why this is the case. Finally, using a phantom gel we demonstrated that photoporation at 800 nm is better suited for transfection of cells located deep in tissues. NIR laser irradiation with fs pulsed lasers from 789 nm to 1554 nm has been tried before to perform photoporation[15,43,44]. For instance, antibody functionalized AuNPs were used as sensitizers to photoporate retinal ganglion cells inside rat eyes in vivo with 800 nm fs pulsed laser irradiation[45]. The authors showed selective delivery of fluorescently tagged siRNAs and FITC-dextrans into retinal cells at a relatively high throughput. However, fs pulsed lasers are rather expensive and complex, limiting its widespread use. In contrast, here we have shown that nanosecond or picosecond pulses are sufficient for efficient photoporation with BPQDs as sensitizers. Therefore, combined with good biocompatibility of BPQDs, it has good potential for translation towards clinical applications requiring deep tissue photoporation of cells in vivo.

4 Conclusions

We have demonstrated for the first time that BPQD are suitable sensitizers for photoporation of cells. Thanks to their extended uniform absorption profile they offer the possibility to perform photoporation not only with laser irradiation in the visible range (532nm), but also in the near infrared range (800nm). We have demonstrated successful photoporation in adherent (Hela and H1299-eGFP) as well as suspension cells (Jurkat) with macromolecules from 10 KDa to 500 KDa. Furthermore, we demonstrated successful intracellular delivery in the presence of a thick phantom gel (2 mm) in the optical path, showing that the delivery efficiency reduced less with NIR irradiation (1.3×) as compared to visible irradiation (2×). This opens up the possibility to perform photoporation of cells deep in tissues, which is expected to facilitate translation of photoporation for in vivo applications.

Conflicts of interest

There are no conflicts to declare.

Author Contribution

J.W., Z.T., R.X. and K.B. conceived and designed the study for using BPQDs for photoporation. Y.W. , X.J. and A.H. were involved in BPQD functionalization and characterization. T.B., J.M.M. and R.X. designed and built the optical instruments for photoporation. J.C.F. was involved in the experiments with gold nanosensitizers. All authors discussed the experiment results and contributed to the manuscript writing.

Acknowledgements

The South China Normal University is acknowledged the financial support by the National Natural Science Foundation of China (No. 61575067). The Centre for Advanced Light Microscopy at Ghent University is acknowledged for the use of its microscopy facilities. Funding by the European Research Council (ERC) under the European Union's Horizon 2020 research and innovation program (Grant 648124) is highly appreciated. J.C.F. and R.H. gratefully acknowledges The Flemish Research Foundation (Grants 1210120N, 1500418N and 12Q8718N). Financial support by the National Natural Science Foundation of China (No. 21774060, 21644004) is acknowledged with gratitude as well

Notes and references

1 M. P. Stewart, A. Sharei, X. Ding, G. Sahay, R. Langer and K. F. Jensen, *Nature*, 2016, **538**, 183–192.

2 L. B. Couto and K. A. High, *Curr Opin Pharmacol*, 2010, **10**, 534–542.

3 J.-S. Lee, J. J. Green, K. T. Love, J. Sunshine, R. Langer and D. G. Anderson, *Nano Lett.*, 2009, **9**, 2402–2406.

4 J. W. Gordon, G. A. Scangos, D. J. Plotkin, J. A. Barbosa and F. H. Ruddle, *PNAS*, 1980, **77**, 7380–7384.

5 B. Gu, E. Posfai and J. Rossant, *Nat. Biotechnol.*, 2018, **36**, 632–637.

6 Y. Cao, E. Ma, S. Cestellos-Blanco, B. Zhang, R. Qiu, Y. Su, J. A. Doudna and P. Yang, *PANS*, 2019, **116**, 7899–7904.

7 G. He, J. Feng, A. Zhang, L. Zhou, R. Wen, J. Wu, C. Yang, J. Yang, C. Li and D. Chen, *Nano Lett.*, 2019, **19**, 7201–7209.

8 E. Neumann, M. Schaefer-Ridder, Y. Wang and P. Hofschneider, *EMBO J.*, 1982, **1**, 841–845.

9 E. F. Fynan, R. G. Webster, D. H. Fuller, J. R. Haynes, J. C. Santoro and H. L. Robinson, *PANS*, 1993, **90**, 11478–11482.

10 N.-S. Yang and W. H. Sun, *Nat. Med.*, 1995, **1**, 481–483.

11 Q. Bi, X. Song, A. Hu, T. Luo, R. Jin, H. Ai and Y. Nie, *Chin Chem Lett*, 2020, **31**, 3041–3046.

12 Z. Fan, H. Liu, M. Mayer and C. X. Deng, *PANS*, 2012, **109**, 16486–16491.

13 R. Xiong, K. Raemdonck, K. Peynshaert, I. Lentacker, I. De Cock, J. Demeester, S. C. De Smedt, A. G. Skirtach and K. Braeckmans, *ACS nano*, 2014, **8**, 6288–6296.

14 M. Gao, Y. Xie, S. Wang, S. Shang and X. Lu, *Bioelectrochemistry*, 2021, **140**, 107790.

15 H. He, S. K. Kong, K. Y. Lee, Y. K. Suen and K. T. Chan, *Opt. Lett.*, 2008, **33**, 2961–2963.

16 M. H. Kafshgari, L. Agiotis, I. Largillière, S. Patskovsky and M. Meunier, *Small*, 2021, **17**, 207577.

17 D. Stevenson, B. Agate, X. Tsampoula, P. Fischer, C. T. A. Brown, W. Sibbett, A. Riches, F. Gunn-Moore and K. Dholakia, *Opt. Express*, 2006, **14**, 7125–7133.

18 U. K. Tirlapur and K. K?Nig, *Nature*, 2002, **418**, 290–291.

19 J. Liu, R. Xiong, T. Brans, S. Lippens, E. Parthoens, F. C. Zanacchi, R. Magrassi, S. K. Singh, S. Kurungot and S. Szunerits, *Light Sci. Appl.*, 2018, **7**, 1–10.

20 L. Raes, S. Stremersch, J. C. Fraire, T. Brans and K. Braeckmans, *Nanomicro Lett*, 2020, **12**, 1–17.

21 L. Raes, C. Van Hecke, J. Michiels, S. Stremersch, J. C. Fraire, T. Brans, R. Xiong, S. De Smedt, L. Vandekerckhove and K. Raemdonck, *Crystals*, 2019, **9**, 411.

22 L. Wayteck, R. Xiong, K. Braeckmans, S. C. De Smedt and K. Raemdonck, *J Control Release*, 2017, **267**, 154–162.

23 R. Xiong, K. Raemdonck, K. Peynshaert, I. Lentacker, C. I. De, J. Demeester, S. C. De Smedt, A. G. Skirtach and K. Braeckmans, *Acs Nano*, 2014, **8**, 6288–6296.

24 A. M. Smith, M. C. Mancini and S. Nie, *Nat. Nanotechnol.*, 2009, **4**, 710–711.

25 C. Yao, F. Rudnitzki, Y. He, Z. Zhang, G. Hüttmann and R. Rahmanzadeh, *J Biophotonics*, 2020, **13**, 1–10.

26 A. M. Alkilany, P. K. Nagaria, C. R. Hexel, T. J. Shaw, C. J. Murphy and M. Wyatt, *Small*, 2010, **5**, 701–708.

27 C. J. Murphy, A. M. Gole, S. E. Hunyadi and C. J. Orendorff, *Inorg. Chem.*, 2006, **45**, 7544–7554.

28 C. Sun, L. Wen, J. Zeng, Y. Wang, Q. Sun, L. Deng, C. Zhao and Z. Li, *Biomaterials*, 2016, **91**, 81–89.

29 J. Shao, H. Xie, H. Huang, Z. Li, Z. Sun, Y. Xu, Q. Xiao, X.-F. Yu, Y. Zhao and H. Zhang, *Nat. Commun.*, 2016, **7**, 1–13.

30 G. Wang, W. J. Slough, R. Pandey and S. P. Karna, *2D Mater.*, 2016, **3**, 025011.

31 T. Zhang, Y. Wan, H. Xie, Y. Mu, P. Du, D. Wang, X. Wu, H. Ji and L. Wan, *J.Am.Chem.Soc.*, 2018, **140**, 7561–7567.

32 D. Lapotko, *Opt. Express*, 2009, **17**, 2538–2556.

33 J. Ramon, R. Xiong, S. Smedt, K. Raemdonck and K. Braeckmans, *Curr Opin Colloid Interface Sci*, 2021, **54**, 101453.

34 J. Liu, J. C. Fraire, S. Smedt, R. Xiong and K. Braeckmans, *Small*, 2020, **16**, 2000146.

35 P. Chakravarty, W. Qian, M. A. El-Sayed and M. R. Prausnitz, *Nature Nanotechnology*, 2010, **5**, 607–611.

36 T. Guo, Y. Wu, Y. Lin, X. Xu, H. Lian, G. Huang, J. Liu, X. Wu and H. Yang, *Small*, 2018, **14**, 1702815.

37 P. Nakhanivej, X. Yu, S. K. Park, S. Kim, J.-Y. Hong, H. J. Kim, W. Lee, J. Y. Hwang, J. E. Yang and C. Wolverton, *NAT MATER.*, 2019, **18**, 156–162.

38 Y. C. Shin, S.-J. Song, Y. B. Lee, M. S. Kang, H. U. Lee, J.-W. Oh and D.-W. Han, *Biomaterials research*, 2018, **22**, 1–8.

39 W. Tao, X. Zhu, X. Yu, X. Zeng, Q. Xiao, X. Zhang, X. Ji, X. Wang, J. Shi and H. Zhang, *Adv. Mater.*, 2017, **29**, 1603276.1–1603276.9.

40 J. Liu, C. Li, T. Brans, A. Harizaj, V. Shana, T. D. Beer, S. D. Smedt, S. Szunerits, R. Boukherroub and R. Xiong, *Int. J. Mol. Sci.*, 2020, **21**, 1540.

41 R. Xiong, S. K. Samal, J. Demeester, A. G. Skirtach, S. D. Smedt and K. Braeckmans, *ADV PHYS-X*, 2016, **1**, 596–620.

42 R. Xiong, R. X. Xu, C. Huang, S. D. Smedt and K. Braeckmans, *Chem. Soc. Rev.*, 2021, **50**, 5746–5776.

43 T. Maeno, T. Uzawa, I. Kono, K. Okano, T. Iino, K. Fukita, Y. Oshikawa, T. Ogawa, O. Iwata and T. Ito, *Sci. Rep.*, 2018, **8**, 1–9.

44 B. H. Naick, A. S. Rao, V. S. Sravanthi, S. Alok and R. Baskaran, *J Photochem Photobiol B*, 2018, **187**, 35–40.

45 A. M. Wilson, J. Mazzaferri, R. Bergeron, S. Patskovsky and P. Sapieha, *Ann. For. Sci.*, 2018, **3**, AB034.